The Plant Cell, Vol. 5, 1541–1553, November 1993 © 1993 American Society of Plant Physiologists

Transposon-Induced Inversion in Antirrhinum Modifies *nivea* Gene Expression To Give a Novel Flower Color Pattern under the Control of *cycloidea*^{radialis}

Clare Lister, David Jackson,[1] and Cathie Martin[2]

Department of Genetics, John Innes Institute, John Innes Centre, Colney Lane, Norwich NR4 7UH, United Kingdom

The *nivea* (*niv*) gene of *Antirrhinum majus* encodes chalcone synthase, an enzyme involved in synthesis of anthocyanin pigments. The *niv*^{rec}:98 allele contains a single copy of the transposon Tam3 inserted at the *niv* locus. A large chromosomal rearrangement derived from this mutant has been shown to be flanked by two copies of Tam3. In this study, we compared sequences involved in this rearrangement with their progenitor sequences and concluded that the rearrangement is an inversion resulting from an aberrant transposition occurring shortly after replication of Tam3 that left both copies of Tam3 active after the rearrangement. Excision of Tam3 from its position adjacent to the *niv* coding region resulted in a novel distribution of anthocyanin pigment in the flower tube, caused by the interaction of the new sequences with the remnant of the *niv* promoter. The new sequences upstream of *niv* serve both to enhance *niv* transcription and to redirect the pattern of gene expression, placing *niv* under the control of the gene *cycloidea*^{radialis}, which determines the morphogenetic polarity of the flower.

INTRODUCTION

Plant transposable elements are well known for their ability to cause chromosomal rearrangements, including deletions, inversions, and duplications. Tam3 in *Antirrhinum majus* induces all these types of rearrangement (Coen and Carpenter, 1988; Martin et al., 1988; Lister and Martin, 1989; Martin and Lister, 1989; Robbins et al., 1989; Hudson et al., 1990). Most of these rearrangements seem to result from transposition-related events rather than from processes involving recombination.

The phenotypically unstable line JI:98 contains Tam3 inserted at *nivea* (*niv*, the locus encoding the enzyme chalcone synthase) (Sommer et al., 1985; Carpenter et al., 1987). Chalcone synthase is the first committed enzyme of flavonoid biosynthesis, and the insertion of Tam3 in this line gives rise to palely pigmented flowers (caused by the transposon inhibiting *niv* expression) with darker sites and sectors that result from somatic excision of the transposon.

A *niv* allele, *niv*^{rec}:531, directly derived from *niv*^{rec}:98, gives rise to flowers with a slightly paler pigmentation than those of its progenitor and retains the unstable phenotype (Carpenter et al., 1987; Martin et al., 1988), as shown in Figure 1. This slight phenotypic difference suggested that a rearrangement had occurred that modified *niv* expression without affecting the ability of Tam3 to excise. We have already shown that this rearrangement involved two copies of Tam3, each one flanked by part of the *niv* locus, and that both copies remain able to excise (Martin et al., 1988). Here, we show that this rearrangement is an inversion generated by Tam3, which also involves duplication of the element. We present a scheme to explain the generation of this type of inversion, based on an aberrant transposition, which requires the close association of both ends of the transposon throughout transposition.

Insertion of Tam3 in the *niv* promoter reduces *niv* expression in the flower lobes and at the base of the flower tubes and completely blocks it in the upper part of the tube, resulting in flowers with palely pigmented lobes and colorless upper tubes (Carpenter et al., 1987). We present evidence that this effect is due to the physical separation by Tam3 of upstream regulatory sequences from the sequences around the TATA box at the *niv* locus, because the same effect is observed when the upstream sequences are deleted by imprecise transposon excision. Excision of Tam3 from its position adjacent to the *niv* coding region in the inversion allele *niv*^{rec}:531 places new sequences (derived from the inversion) upstream of the *niv* TATA box and coding sequence. These sequences result in a higher level of *niv* expression than when the *niv* upstream sequences are deleted and also give rise to a novel color pattern phenotype resulting from the *niv* gene being expressed on the adaxial side of the upper flower tube but not the abaxial side. This novel pattern of expression, responding to flower polarity, appears to be under the control of the gene *cycloidea*^{radialis} (*cyc*^{rad}), which is required for bilateral symmetry

[1] Current address: U.S. Department of Agriculture, Plant Gene Expression Center, 800 Buchanan Street, Albany, CA 94710.

[2] To whom correspondence should be addressed.

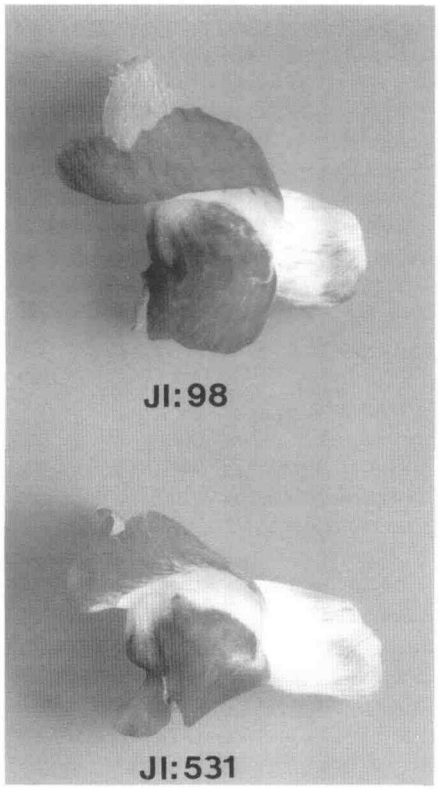

Figure 1. Phenotypes of the Progenitor *niv*^{rec}:98 Allele and of the Derivative Allele *niv*^{rec}:531.

On top is JI:98, below is JI:531. *niv*^{rec}:531 gives darker sites on a palely pigmented background. The sites in *niv*^{rec}:531 are paler than those for *niv*^{rec}:98.

of the flower. In *cyc*^{rad} mutants, all petals develop as "lower" petals to give a radially symmetrical corolla. The establishment of a *niv* allele responding to *cyc*^{rad} as a result of alteration of the *niv* promoter suggests that *cyc* controls petal determination and hence floral symmetry either directly or indirectly by regulating gene transcription.

RESULTS

Identification of the *niv*^{rec}:531 Allele

Tam3 has been inserted 64 bp upstream of the start of *niv* transcription in the *niv*^{rec}:98 allele of JI:98 (Sommer et al., 1985). DNA probes from the *niv* gene, containing the sequences upstream (probe A) or downstream (probe B) of the insertion site of Tam3 at *niv*, were used to map the *niv*^{rec}:531 allele (Martin et al., 1988). Hybridization of probe A to *niv*^{rec}:531 genomic DNA digested with EcoRI (which does not cut within Tam3) revealed a new EcoRI fragment of 10.5 kb, compared to the 9.2-kb fragment of *niv*^{rec}:98. Hybridization of probe B to the same DNA gel blot revealed a second new EcoRI fragment of 12.5 kb. This indicated that the upstream promoter sequences (A) and coding regions (B) of *niv* were still present in the genome but were no longer adjacent to each other. Martin et al. (1988) showed that in *niv*^{rec}:531, these two fragments cosegregate and are therefore linked. This suggested that the rearrangement might be an inversion.

niv^{rec}:531 causes a somatically unstable (*recurrens*) pigment phenotype, indicating that Tam3 remains adjacent to the coding sequence (B) of *niv*. Restriction mapping of genomic DNA had confirmed this and had also shown that a second copy of Tam3 remains adjacent to the promoter region (A) (Martin et al., 1988). The detection of somatic and germinal excision bands in EcoRI-digested genomic DNA of 7 kb (homologous to region A) and 9 kb (homologous to region B), both 3.5 kb smaller than their progenitor 10.5- and 12.5-kb bands, respectively, indicated that both copies of Tam3 remain able to excise somatically and germinally, and the isolation of germinal excisions of Tam3 adjacent to region A or of Tam3 adjacent to region B showed that each Tam3 copy could excise independently (Martin et al., 1988).

Cloning and Mapping of the *niv*^{rec}:531 Allele

To isolate the two parts of the *niv* locus in *niv*^{rec}:531, a library was prepared by partial EcoRI digestion of JI:531 genomic DNA and cloning in λ EMBL4 (see Methods). Two clones containing *niv* sequences were isolated.

One contained a 7.0-kb EcoRI fragment that hybridized to probe A but not to probe B or Tam3. This clone contained the upstream *niv* promoter sequences (A), with new adjacent sequences (termed *y*), but Tam3 was not present; this clone, therefore, represented a somatic excision of Tam3. The other clone contained a 12.5-kb EcoRI fragment that hybridized to probe B and Tam3 but not to probe A. This clone, therefore, contained the *niv* coding sequence, in addition to Tam3 and new adjacent sequences (termed *z*). The relevant EcoRI fragments from these two clones were subcloned into pUC18 to yield the plasmids pAy and pBT3z, as shown in Figures 2A and 2B.

Cloning and Mapping of the Progenitor Sequence *yz* from JI:98

If the rearrangement in *niv*^{rec}:531 had been an inversion, then both new sequences (*y* and *z*), adjacent to the *niv* upstream promoter sequences (A) and coding regions (B), respectively, should have been present originally on a single EcoRI restriction fragment in the progenitor line JI:98. A genomic library of JI:98 DNA prepared by partial digestion with EcoRI and cloned into λ EMBL4 was screened with pAy. One clone contained a 10.0-kb EcoRI fragment that hybridized to both pAy and pBT3z. This 10.0-kb fragment was subcloned into pUC18 digested with EcoRI to yield pyz.

To confirm that this plasmid contained sequences from both region *y* and region *z*, double digestions were performed (EcoRI plus enzymes known to cut in either *y* or *z*) on pyz, pAy, and pBT3z. This showed that bands in pyz comigrated with bands in both of the other two plasmids. A restriction map of this clone could then be drawn (Figure 2B). Sequences *y* and *z* are, therefore, found to be adjacent and on the same restriction fragment in the progenitor line JI:98. The fact that regions *y* and *z* were located on the same EcoRI fragment in the progenitor as well as these regions' relative orientations confirmed that the rearrangement at *niv*^{rec}:531 was an inversion.

An inversion flanked by two copies of a transposable element could be formed by recombination between two copies of the element in an inverted orientation, leading to an inversion of the intervening sequence (Kleckner and Ross, 1980; Roeder and Fink, 1983). It was clear from the restriction map of pyz (Figure 2B) and hybridization data that a copy of Tam3 was not present at this locus in the progenitor line. Genomic DNA from the actual parental plant that gave rise to the inversion among its progeny was mapped using restriction enzymes and did not show a copy of Tam3 to be resident at *yz* (C. Lister, unpublished data). Unless the insertion of Tam3 at *yz* was an extremely brief somatic encounter, it is very unlikely that this inversion arose by recombination, and we favor the view that it arose through aberrant transposition.

Sequence Analysis of pyz, pAy, and pBT3z

The DNA sequence at the break point of the inversion was determined, as shown in Figure 3A. To establish how the inversion was generated, we also determined the sequence

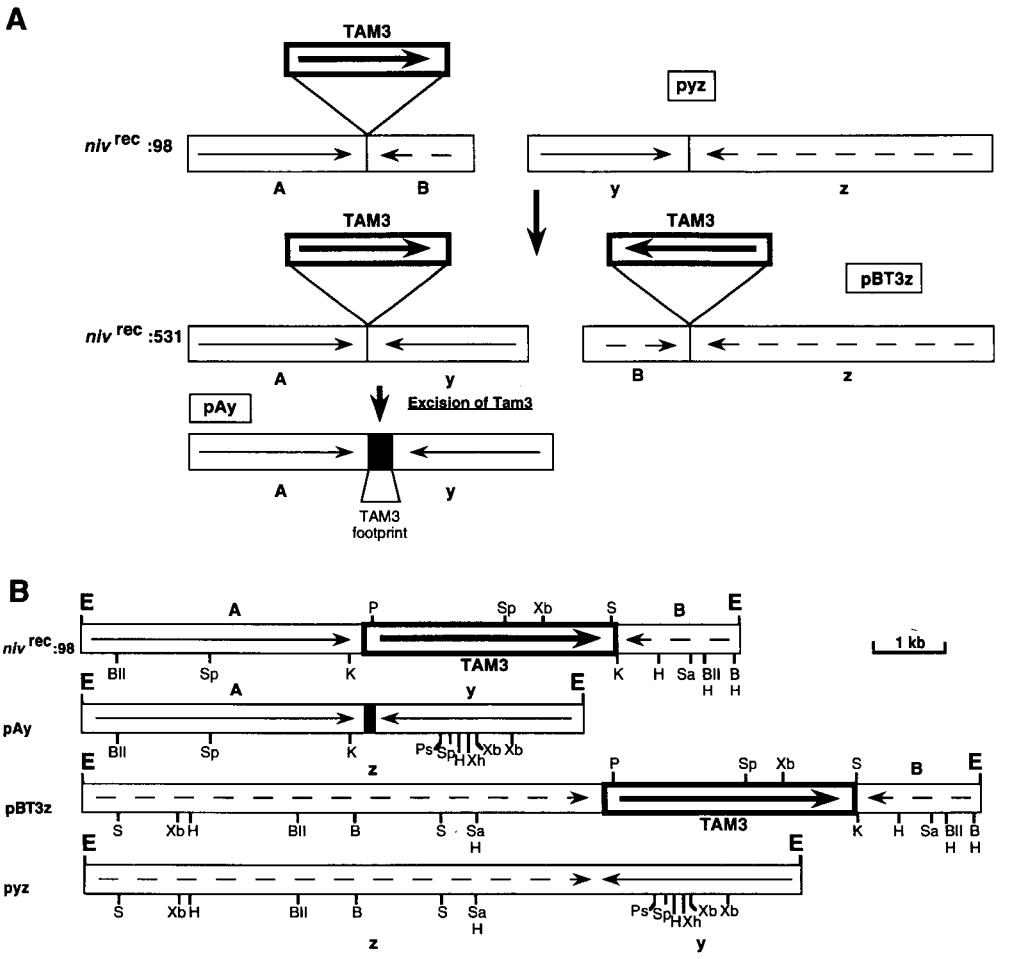

Figure 2. Diagram and Restriction Enzyme Maps of the *niv* and *yz* Loci in *niv*^{rec}:98 and *niv*^{rec}:531.

(A) Diagram of the structures of *niv* locus and reciprocal locus *yz* in the progenitor line *niv*^{rec}:98 and in the inversion line *niv*^{rec}:531 The relative orientation of each DNA fragment and each copy of Tam3 is indicated by arrows. The plasmid names for each fragment are indicated, including the somatic excision of Tam3 from Ay (pAy). A and B indicate probes A and B.

(B) Restriction maps of the *niv* locus in *niv*^{rec}:98, pAy, pBT3z, and pyz. B, BamHI; BII, BglII; E, EcoRI; H, HindIII; K, KpnI; Ps, PstI; P, PvuII; S, SmaI; Sa, SalI; Sp, SphI; Xb, XbaI; Xh, XhoI. Arrows indicate the relative orientation of fragments, as indicated in **(A)**.

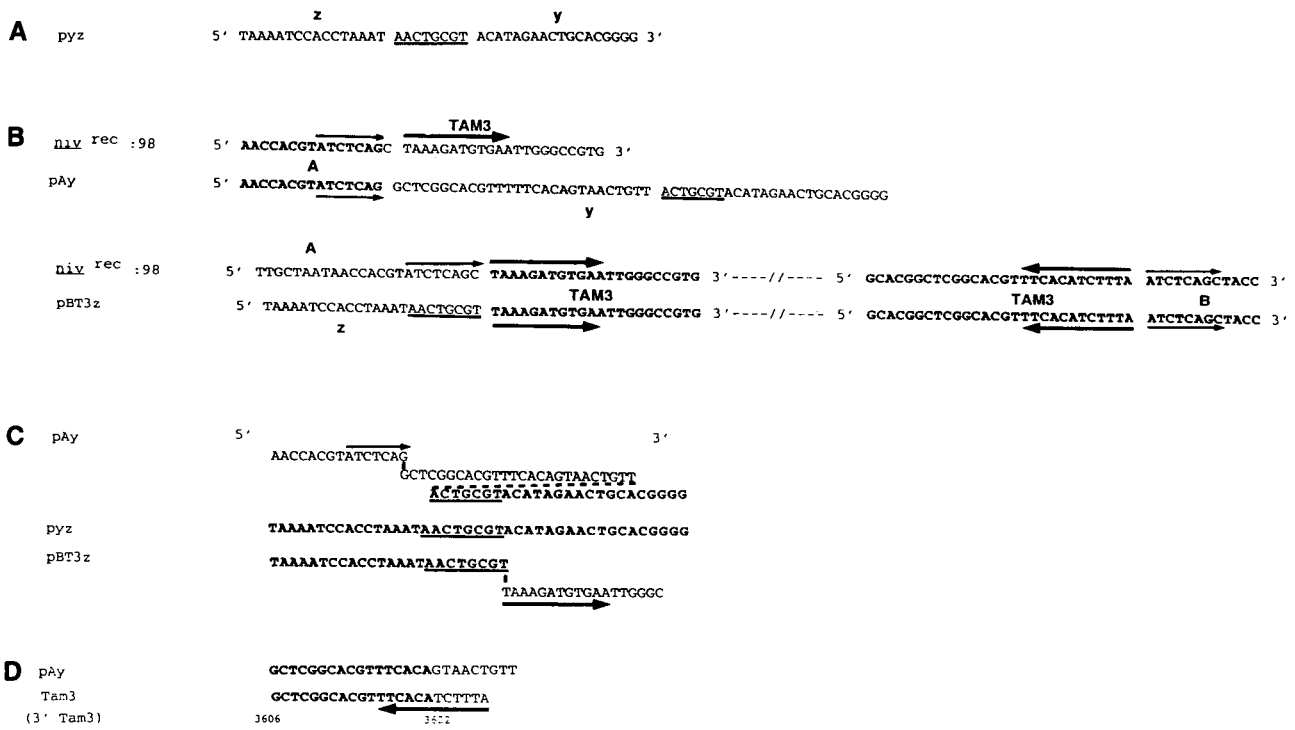

Figure 3. Sequences of the Ends of the Inversion in *niv*^{rec}:531.

(A) Sequences of the region spanning the break point of the inversion at the progenitor locus, *yz*, in pyz. Bases duplicated in the rearrangement are underlined.

(B) Comparison of the sequences around the break points of the inversion in pAy and pBT3z with those of *niv*^{rec}:98 (Sommer et al., 1985). Light arrows indicate the bases duplicated at *niv* and heavy arrows the inverted termini of Tam3. Bases duplicated in the rearrangement are underlined.

(C) Amalgamation of the sequence data from **(A)** and **(B).** The light arrow indicates the bases duplicated at *niv*, and the heavy arrows indicate the inverted termini of Tam3. The bases duplicated on formation of the inversion are underlined; the dashed line represents continuation of the sequence.

(D) Comparison of the sequence of the insertion in pAy with the 3' end of Tam3. The arrow indicates the inverted termini of Tam3. Numbers indicate the position in the Tam3 sequence (Hehl et al., 1991).

across the boundary between *niv* fragment A and *y* in pAy and the sequences between Tam3 and *niv* fragment B and Tam3 and *z* in pBT3z.

Clone pAy represents a somatic excision of Tam3 from the insertion site adjacent to the upstream *niv* promoter sequences. The DNA sequence across the junction between A and *y* was determined (Figure 3B) and compared to the *niv* sequence from *niv*^{rec}:98. The *niv* sequence upstream from the former Tam3 insertion site in pAy was exactly as in *niv*^{rec}:98, except that 1 bp was missing from the 8-bp direct duplication generated by Tam3 on insertion in the *niv* locus (Sommer et al., 1985). Further downstream from this excision, the sequence was completely different from that of *niv*^{rec}:98.

The B sequences adjacent to the 3' end of Tam3 in pBT3z and the sequence at this end of the element were exactly the same as that of *niv*^{rec}:98 (Figure 3B), indicating that both Tam3 and the *niv* sequences flanking this end of the element were not disturbed during the formation of this rearrangement.

The sequence at the junction between the 5' end of Tam3 and region *z* in pBT3z (Figure 3B) showed that the copy of Tam3 adjacent to the *niv* coding sequence in *niv*^{rec}:531 had inverted termini identical to those of the copy of Tam3 in *niv*^{rec}:98, confirming that the former was most probably derived from the latter (because sequence variation between different copies of Tam3 has been previously observed; Martin et al., 1989). Beyond Tam3, the sequence of pBT3z was completely different from that of the *niv* promoter (A) in *niv*^{rec}:98.

The relevant sequence data from Figures 3A and 3B are combined in Figures 3C and 3D. This shows that a 7-bp sequence (ACTGCGT) at the site of the break point in the progenitor (pyz) is found in region *y* in pAy and in region *z* in pBT3z. The duplication was probably originally 8 bp (AACTGTGT), with an A residue being lost when Tam3 excised (Tam3 generates either 5- or 8-bp duplications upon insertion: Sommer et al., 1985; Coen et al., 1986; Martin et al., 1989). These duplications, therefore, suggest "attempted" Tam3 integration at *yz*, although Tam3 did not concomitantly excise from *niv*, supporting the view that the inversion was generated during an aberrant transposition.

Comparison of the sequences from pAy and pBT3z with those of the progenitor pyz was expected to show a continuity of sequence between regions *y* and *z*. However, we found a

26-bp insertion between the promoter region (A) of *niv* and *y* in pAy (Figure 3C) that we believe to be part of the transposon footprint generated during the somatic excision of Tam*3* (Sommer et al., 1985; Martin and Lister, 1989). Comparison of the sequence of this insertion with that of Tam*3* shows that 17 bp are homologous to a small region of the element, which is close to the 3′ end (Figure 3D), showing that sequences internal to the element were involved in generating its footprint during excision.

Linkage Analysis of *niv* and *yz*

The isolation of regions *y* and *z* on a single restriction fragment from the progenitor line confirmed that the rearrangement that gave rise to *niv*^{rec}:531 was an inversion. This also implies that *niv* and *yz* are linked. The distance between the two points was determined by linkage analysis, using the F_2 progeny of a cross between two laboratory lines, JI:98 and JI:5A (Lister and Martin, 1989), which showed restriction fragment length polymorphisms (RFLPs) with EcoRI for both *yz* and *niv* probes. Genomic DNAs from 33 homozygous *niv*^{rec} F_2 plants were digested with EcoRI and hybridized to pyz. Thirty-two of the homozygous *niv*^{rec} F_2 plants were also homozygous for the JI:98 polymorphism at *yz*, and only one plant was a heterozygote. The recovery of only one recombinant indicates that *niv* and *yz* are very closely linked (1.5 centimorgans [cM]) (Martin and Lister, 1989); *yz* has subsequently been placed on the Antirrhinum RFLP map and has been estimated to lie 12 cM from *niv* (Z. Schwarz-Sommer, personal communication). These differences in estimated map distances probably result from the fact that the RFLP map is based on a species cross (*A. majus* × *A. molle*), whereas our initial mapping used closely related lines, because map distances between genetic markers are known to vary between *Antirrhinum* spp (Stubbe, 1966). The distance of 1.5 cM is, therefore, more reliable in assessing the attempted transposition of Tam*3* in the generation of *niv*^{rec}:531.

Phenotypes of Excisions of Tam*3* from *niv*^{rec}:531

In the allele *niv*^{rec}:98, Tam*3* is situated in the *niv* promoter, which is 64 bp upstream of the start of transcription in a region that is important for the control of *niv* expression (Sommer et al., 1985, 1988a; Kaulen et al., 1986; Sommer and Saedler, 1986; Lipphardt et al., 1988; Schulze-Lefert et al., 1989a, 1989b). When Tam*3* is stably inserted (for example, in plants grown at 25°C or homozygous for the *Stabiliser* locus), the overall intensity of the anthocyanin in the lobes is reduced. No color is detected in the upper part of the flower tube (Carpenter et al., 1987), as shown in Figure 4B. These changes result from reductions in *niv* gene expression that make it the rate-limiting step in anthocyanin biosynthesis following displacement of upstream *niv* promoter sequences away from the 63-bp remnant of the *niv* promoter. The influence of the sequences upstream of −63 bp on *niv* expression in the flower is also observed in imprecise excisions of Tam*3*, such as one that removes 1027 bp of sequence from −64 to −1091 inclusive in *niv*:593 (Figure 4C), and in a second inversion generated by Tam*3*, *niv*:566, which replaces all sequences upstream of the Tam*3* insertion site with a novel sequence (Martin et al., 1988; Martin and Lister, 1989). The phenotypic consequences of loss or displacement of these upstream elements are therefore identical.

The inversion in *niv*^{rec}:531 also displaces the sequences upstream of −63 bp in the *niv* promoter but does not give the expected pale phenotype in plants in which Tam*3* has excised.

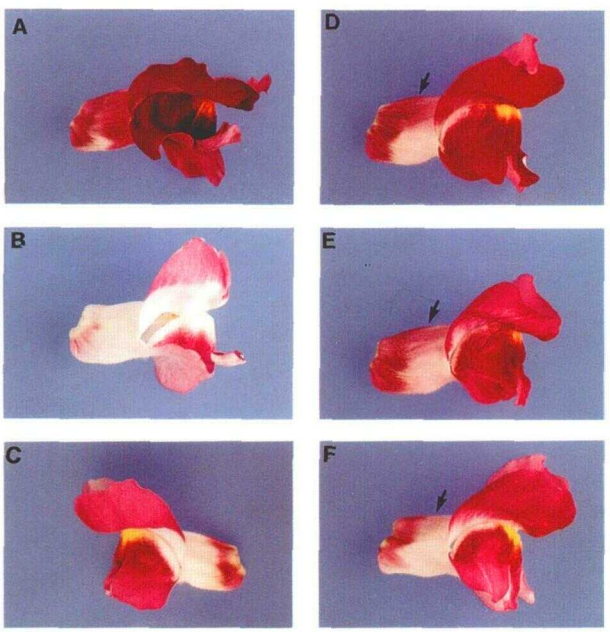

Figure 4. Phenotypes of Flowers from Lines with Tam*3*-Induced Rearrangements of the *niv* Promoter.

(A) Wild type (JI:7) with normal *niv* promoter showing high pigmentation in the lobes and a relatively uniform pigmentation of the flower tube.
(B) JI:558. As in JI:98, Tam*3* lies 64 bp upstream of the start of *niv* transcription, but somatic excision is suppressed in this line by the *Stabiliser* locus (Harrison and Fincham, 1968; Carpenter et al., 1987). The phenotype reflects the effect of displacement of the normal *niv* sequences upstream of −63 bp (by the insertion of the transposon) so that they no longer direct *niv* expression. Pigmentation is reduced in the tube lobes and is absent from the upper part of the tube as a result of altered *niv* expression. This phenotype represents the effect of the loss of sequences upstream of −63 bp on *niv* expression shown in **(C)**.
(C) *niv*:593. The phenotype observed after a 1027-bp deletion of sequence from −64 to −1090 inclusive in the *niv* promoter shows a dramatic reduction in pigmentation of the lobes and an absence of pigmentation in the upper tube.
(D) to **(F)** Phenotypes of lines derived from *niv*^{rec}:531 following Tam*3* excision. Pigmentation caused by *niv* expression is high in the lobes of **(D)** *niv*:531R1, **(E)** *niv*:531R2, and **(F)** *niv*:531R3, and a new pattern of pigmentation, a broad stripe of pigmentation along the adaxial side of the tube (arrow), is also observed most clearly in **(D)** and **(E)** and also faintly in **(F)**.

Three independent germinal excisions of Tam3 from between region z and the *niv* coding region were identified (*niv*:531R1, *niv*:531R2, and *niv*:531R3) by selection for a stable flower color phenotype. Plants carrying these alleles were selfed to produce lines homozygous for the excision events. The floral pigmentation in these *niv*:531 revertants was higher in the lobes than would be predicted from a "neutral" change (i.e., one involving displacement and functional loss of the upstream sequences of the *niv* promoter). There was also a novel distribution of pigment in the tube. These flowers showed a broad stripe of pigmentation on the upper or adaxial surface of the tube but no pigmentation on the lower or abaxial surface (Figures 4D to 4F). Such a stripe of pigment is not seen on a wild-type flower, in which the tube pigmented on both sides (Figure 4A), or in the progenitor JI:98, and it is also not seen in other lines that have lost the upstream promoter sequences (such as JI:593), with no pigment being observed in the upper part of the tube (Figure 4C). The phenotype of these more darkly pigmented flowers suggests that, on excision of Tam3 from *niv*^{rec}:531, the new sequence (z) not only enhances *niv* gene expression in the flower lobes but also contains motifs that promote *niv* expression in the upper part of the tube.

DNA Sequence Determination of the Excision Alleles from *niv*^{rec}:531

The alleles derived from Tam3 excision from *niv*^{rec}:531 were analyzed to provide information on the changes in *niv* gene expression. Polymerase chain reaction (PCR) was used to amplify the required sequences from genomic DNA, as shown in Figure 5. The excisions of Tam3 from *niv*:531R1 and *niv*:531R2 were identical. One base pair was deleted both from the 8-bp duplication of *niv* sequence and from region z, and 2 bp (AC) were added at the excision site. These excisions, therefore, did not remove any of the sequences known to be important for *niv* gene expression downstream of the insertion site of Tam3 (Sommer et al., 1988a). The sequence data obtained from *niv*:531R3 show that 11 bp of *niv* sequence were deleted, including the 8-bp transposon-induced duplication and part of the TACCAT motif closest to the insertion site of Tam3. The lower level of pigmentation in JI:531R3 lines carrying this allele (Figure 4F) compared to JI:531R1 and JI:531R2 (Figures

Figure 5. DNA Sequence Data Obtained from the Excision Alleles *niv*:531R1, *niv*:531R2, and *niv*:531R3.

The sequences obtained from *niv*:531R1, *niv*:531R2, and *niv*:531R3 are compared with the sequence of *niv*^{rec}:531 (zB). The arrow indicates the bases duplicated at *niv* by transposon insertion. Underlined bases indicate the TACCAT motifs known to be required for high-level expression of *niv*. Bases shown as lowercase letters are additional bases that are a result of excision.

4D and 4E) indicates a lower level of *niv* expression. The duplicated TACCAT motifs in the *niv* promoter have already been shown to determine the level of *niv* gene expression (Sommer et al., 1988a), and from these results they appear to operate in the context of a new chimeric *niv* promoter as well. In *niv*:531R3, 1 bp was deleted from region z, and 6 bp (ACGCAT) were added between z and *niv*.

The changes in *niv* expression driven by the chimeric promoter and formed from the combination of region z with 62 bp of the *niv* promoter remaining upstream of the coding sequence in *niv*:531R2 were examined by RNA gel blotting and in situ hybridization. RNA was extracted from lobes of the wild type, JI:531R2, and JI:593 (for comparison of JI:531R2 with the effect of loss of the *niv* sequences). Loss of the *niv* sequences upstream of −62 bp reduced the steady state levels of *niv* mRNA in lobes ninefold, as shown by comparison between the wild type and *niv*:593 and quantification of transcript levels using scanning densitometry and correction to a ubiquitin standard, as shown in Figure 6A. In *niv*:531R2, however, despite loss of these upstream sequences, the level of *niv* transcript in the lobes was calculated to be 1.7-fold higher than in *niv*:593 after correction to the ubiquitin standard, confirming that the chimeric promoter in *niv*:531R2 provides an enhancement of *niv* expression in the lobes by 70% over the basal level directed by the remnant of the *niv* promoter in *niv*:593. This effect is likely to be due to the provision of binding sites for transcription factors by z rather than by the rearrangement of the binding sites of the general transcriptional machinery, because *niv* transcription initiates at the same point in the wild type, JI:593, and JI:531R2 (Sommer and Saedler, 1986; Figure 6D).

In situ hybridization, as shown in Figure 7, revealed that in wild-type lines *niv* was expressed in both the inner and outer epidermal cells of the lobes, of the adaxial and abaxial sides of the upper tube, and of the base of the tubes. In JI:593, *niv* expression was epidermal specific but not detected on either side of the upper part of the tube. In JI:531R2, *niv* was expressed at a relatively high level in the lobes and at the base of the tube, and transcript was detected in the epidermal cells of the adaxial side of the tube but not in those on the abaxial side. These results confirmed the changes in pigment production and indicated that, in the chimeric promoter, region z could direct both a novel and enhanced pattern of *niv* expression in flowers. These results also showed that sequences downstream of −63 bp must be responsible, in *cis*, for determining the epidermal-specific expression of the *niv* gene in flowers, because expression was maintained in both *niv*:593 (where the sequences between −63 and −1091 bp had been deleted) and in *niv*:531R2, in which all sequences upstream of −62 bp had been displaced.

Role of z in Directing *niv* Expression in the Flower Tube

In excision alleles *niv*:531R1, *niv*:531R2, and *niv*:531R3, *niv* expression was observed in the upper part of the flower tube,

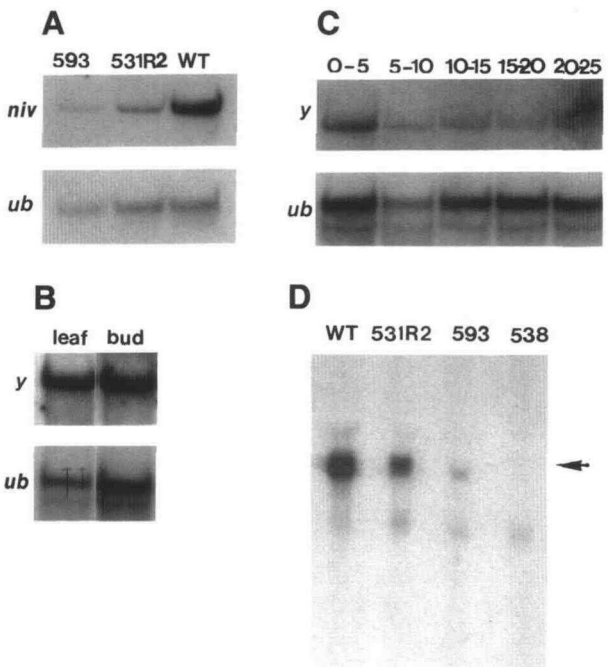

Figure 6. RNA Gel Blot Analysis of Gene Transcription Affected by the *niv*:531 Inversion.

(A) *niv* expression in lobes of the wild type (WT; JI:7), the deletion line JI:593, and the inversion line JI:531R2 showing that the chimeric *z/niv* promoter in JI:531R2 allows higher *niv* expression (~1.7-fold) than the remnant of the *niv* promoter alone (JI:593). The loading of total RNA per track was standardized using a ubiquitin cDNA probe (ub) as a control.

(B) Transcript detected by sequences in region *y* from pyz in 7 μg of poly(A)$^+$ RNA from wild-type leaves and young buds. Ubiquitin (ub) was used as a control.

(C) Expression of the transcript encoded by region *y* from pyz in 7 μg of poly(A)$^+$ RNA from wild-type developing flower buds (sizes of flower buds are indicated in millimeters). Expression was highest in the youngest buds tested (0 to 5 mm long). Ubiquitin (ub) was used as a control.

(D) Primer extension analysis showing that transcription is initiated in *niv* alleles *niv*:531R2 and *niv*:593 in the same position as in the wild-type (WT) *Niv*$^+$ alleles. A *niv*$^-$ null allele, *niv*:538, was used as a control. The arrow indicates extension of the primer by reverse transcriptase corresponding to the transcriptional initiation position identified by Sommer and Saedler (1986).

but only on the adaxial side. This suggested that region *z* might be involved in determining gene expression with respect to the adaxial/abaxial polarity of the flower. To test this further, we used a mutant of Antirrhinum carrying *cyc*^{rad}, which causes the normally zygomorphic flowers to develop with radial symmetry and the two adaxial ("back") petals to develop in the same form as the abaxial lower petals. This may be due to loss of a factor involved in establishing adaxial/abaxial polarity (Carpenter and Coen, 1990). A line homozygous for this mutation (JI:25) was crossed to line JI:531R2, and the *cyc/niv*:531R2 homozygotes segregating in the F_2 generation, which were identified by their radial symmetry and reduced level of pigmentation in lobes compared to *Niv*$^+$, were examined. In this cross, there was incomplete penetrance of the *cyc* phenotype; some flowers of *cyc* homozygotes were completely radially symmetrical, whereas in many plants, varying degrees of partial bilateral symmetry remained.

In F_2 flowers that were completely radially symmetrical, no adaxial stripe of pigmentation in the tube was observed, as shown in Figure 8D. In flowers with some bilateral symmetry, a narrow adaxial band of pigment was seen, reaching from the outer edge of one back petal to the outer edge of the other, whereas in the completely bilaterally symmetrical flowers (*Cyc*$^+$) the normal stripe along the adaxial side of the tube was seen (Figure 8B). This supports the view that *z* contains sequence motifs responding to factors determining whether morphologically distinct back and lower petals develop. This appears to depend on genes, such as *cyc*, that establish the adaxial/abaxial polarity of the flower. Such motifs can probably be bound by transcription factors with this type of polar distribution; in their new position next to the TATA box of the *niv* gene (following the *niv*^{rec}:531 inversion), they can activate *niv* expression in the tube in response to these new directions. To test whether the sequences in region *z* were normally associated with a gene responding to signals in floral morphogenesis, mRNA from leaves and young flower buds from wild-type plants was separated on RNA gel blots, and a transcript of 1.7 kb (Figure 7B) was identified using the sequences of *y* as a probe (a HindIII-HincII fragment from pyz that contains 1.5 kb of region *y* from the HindIII site in region *y* to ~200 bp beyond the Tam3 insertion site; Figure 2B). This transcript was present in leaves and young flower buds, although its expression decreased with the age of the flowers (Figure 6C). These results suggest that the motifs of *z* do normally act as promoter motifs controlling expression of another gene; following the inversion, they would direct *niv* expression in a novel fashion.

DISCUSSION

Generation of Inversions and the Mechanism of Transposition Excision

The *niv*^{rec}:531 allele arose by an inversion that separated the promoter and coding regions of the *niv* gene. There are several possible mechanisms by which a chromosomal inversion might be formed, including recombination between two inverted copies of a transposable element (reviewed for *Ty* elements of yeast by Roeder and Fink, 1983; Boeke, 1989 and described for integrating *I* elements in Drosophila by Busseau et al., 1989) or breakage at or near the site of insertion of two elements, with subsequent inversion of the intervening sequence (described for *P* elements in Drosophila by Engels and Preston, 1984). Because no second copy of Tam3 was present at the reciprocal locus (*yz*), these mechanisms seem very unlikely. This is because the rearrangement would require the consecutive occurrence of two events—integration followed

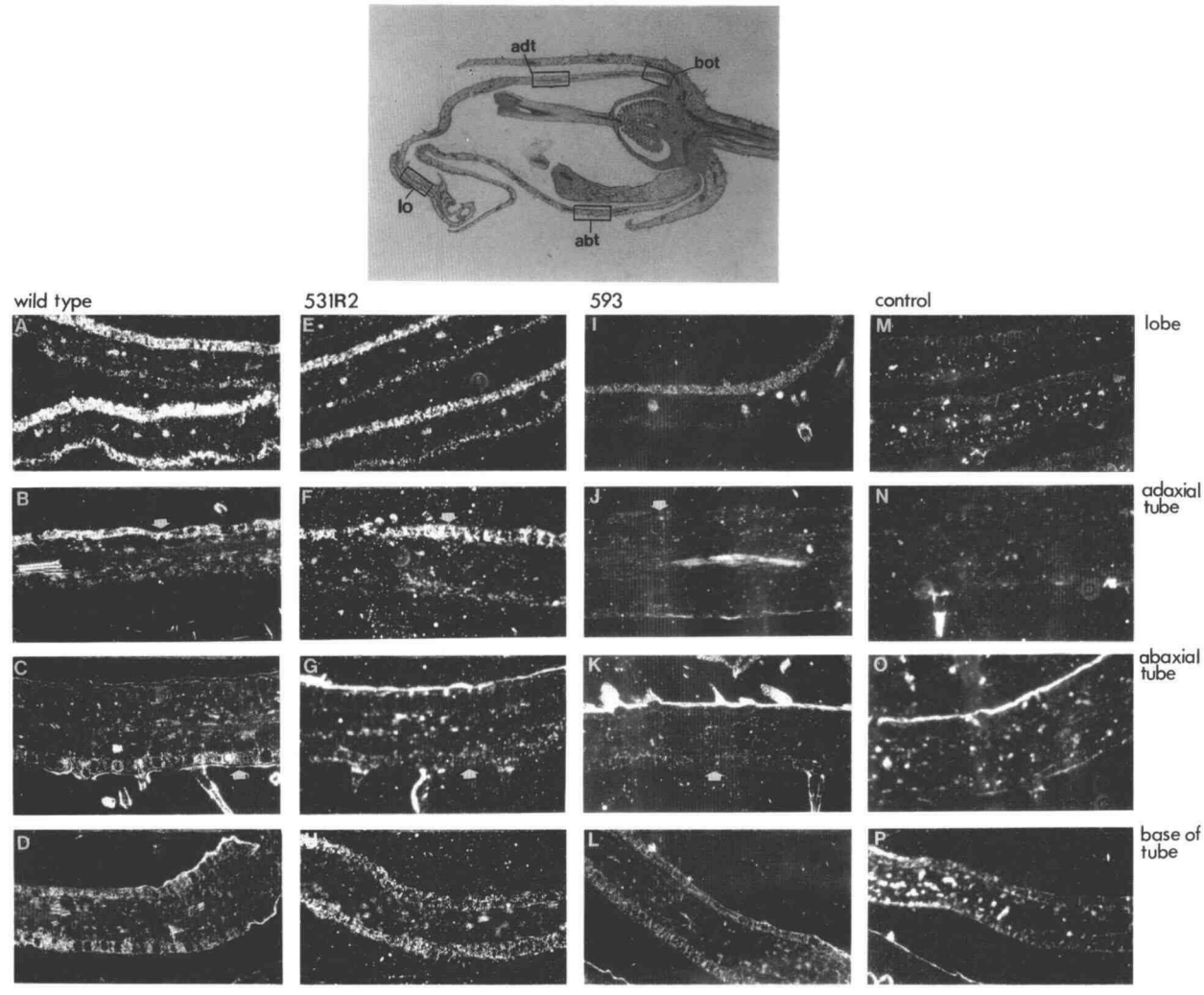

Figure 7. In Situ Hybridization of Antisense *niv* Riboprobe to Flower Petal Sections from Buds 15 to 25 mm Long.

(Upper panel) shows a longitudinal section through a flower bud with the positions of samples illustrating hybridization to the lobes (lo), the adaxial upper tube (adt), the abaxial upper tube (abt), and the base of the corolla tube (bot).
(A) to **(D)** Wild-type (JI:7) flowers. Hybridization to epidermal cells from lobes is shown in **(A)**, adaxial upper tube in **(B)** (arrow), abaxial upper tube in **(C)** (arrow), and the base of the tube in **(D).**
(E) to **(H)** JI:531R2. Expression is shown in the epidermis of lobes **(E)**, adaxial upper tube **(F)** (arrow), and base of the tube **(H)** but not in the abaxial upper tube **(G)** (arrow).
(I) to **(L)** JI:593. Expression is shown in the epidermal cells only of the lobes **(I)** and base of tubes **(L)** and not in the upper tube **(J** and **K)** (arrows).
(M) to **(P)** Control hybridization of the sense *niv* probe to JI:531R2, which shows no hybridization. The brightness of some epidermal layers and vascular tissue under dark-field microcsopy is due to reflection of light by these tissues and not due to precipitated silver grains.

by recombination or chromosome breakage—in a single plant generation. The direct duplication of sequence from *yz* at the ends of the rearrangement is additional evidence that this inversion arose through a transposition-related process.

One model for formation of an inversion at the *pallida* locus (Robbins et al., 1989) proposed that breakage occurs at one end of Tam*3* and that the free end ligates with a recipient site, without subsequent breakage and transfer of the other end of the element, thus leading to inversion of the intervening sequence. This model cannot explain the inversion of sequence in *niv*^{rec}:531 because it does not account for the presence of two copies of Tam*3*, which are derived from the single progenitor element at *niv* (Martin et al., 1988). We suggest that DNA replication generated the two Tam*3* copies, followed by transposition. However, because the transposition was aberrant, the intervening sequence between *niv* and *yz* became

inverted, as shown in Figure 9. We propose that in a normal transposition, transposase-induced breaks occur at each end of a newly replicated element, followed by transfer of the ends of the element to a new insertion site, often closely linked (Figure 9). This supports the conclusions of Hudson et al. (1990), who examined another *niv* allele derived from *niv*^{rec}:98 that contained two copies of Tam3 that were located in new positions within 3 kb on either side of the former insertion site. The maize transposon *Activator* (known to be structurally related to Tam3: Sommer et al., 1988b; Hehl et al., 1991) transposes shortly after replication (Greenblatt and Brink, 1962; Chen et al., 1987), preferentially to closely linked chromosomal positions (Van Schaik and Brink, 1959; Greenblatt, 1984; Jones et al., 1990); our data for Tam3 would support the view that structurally related transposons from different species show similar functional traits.

We propose that the inversion of sequence in *niv*^{rec}:531 resulted from an aberrant version of this transposition process. Shortly after replication, breaks occurred at opposite ends of each newly replicated element instead of at the same element. This might have happened if the two sister chromatids were still in close association after replication, so that the transposase complex recognized and caused breakage at one end of one copy of Tam3 and the opposite end of the other element. If the two ends of the different copies of Tam3 integrated at *yz*, then replication of *yz* would result in an inversion of the sequences between *nivea* and *yz* with a copy of Tam3 at each end (Martin and Lister, 1989; Figure 9). A second *niv* allele, *niv*^{rec}:566 (Martin et al., 1988), has the same structure as *niv*^{rec}:531 (an inversion of sequence flanked by two copies of Tam3); this may, therefore, be a common mechanism for generating inversions.

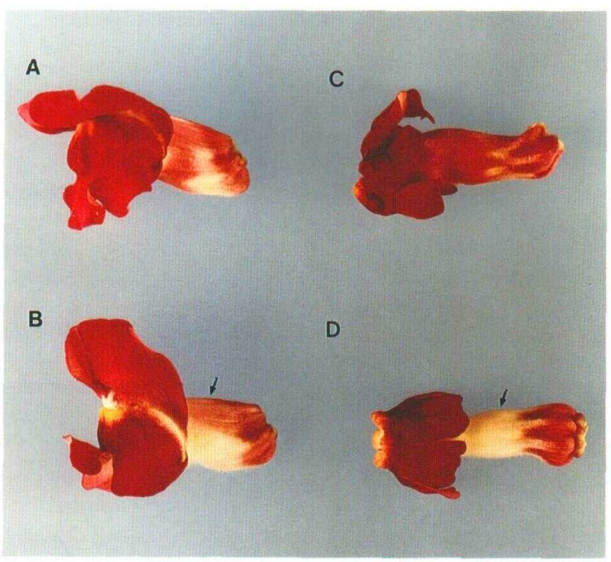

Figure 8. Effect of *cyc*^{rad} on *niv* Expression in the Adaxial Tube Tissue.

(A) *Cyc*$^{+}$ with the wild-type *Niv*$^{+}$ allele. The flowers are bilaterally symmetrical and pigmentation extends right around the upper part of the tube.

(B) *Cyc*$^{+}$ with *niv*:531R2. The flowers are bilaterally symmetrical and the adaxial stripe of tube pigmentation extends to the outer edges of the two back petals (indicated by the arrow).

(C) *cyc* with the wild-type *Niv*$^{+}$ allele. The flowers are completely radially symmetrical and uniformally pigmented in the upper tube.

(D) *cyc* with *niv*:531R2. The flowers are completely radially symmetrical and no adaxial stripe of pigment is observed in the upper part of the tube (the position of which is indicated by the arrow).

This model could explain equally well the formation of the inversion described by Robbins et al. (1989). In the original plant, two copies of Tam3 would have been associated with the rearrangement, one at each end of the inversion. However, in the maintenance of the line, one copy of Tam3 might have excised from one end of the inversion to leave a single copy associated with the *pallida* locus. Aberrant transpositions of Tam3 by this mechanism could also give rise to large-scale deletions, such as *niv*$^{-}$:529 (Lister and Martin, 1989) and *niv*^{rec}:561 (Martin et al., 1988), and smaller adjacent deletions generated by other plant transposons, such as *Mutator* (Taylor and Walbot, 1985) and *Activator* (Dooner et al., 1988). If breakage occurred at opposite ends of the two replicated elements (as described in Figure 9 for the aberrant transposition) and at *yz*, and the copy of the transposon attached to A ligated with *z* instead of *y*, the chromosomal segment containing B, *y*, and the intervening sequence would be lost. The resulting structure would be identical to that observed in deletion alleles such as *niv*$^{-}$:529 and *niv*^{rec}:561. Although it is not possible to prove that these inversions and deletions did not arise through recombination between dispersed Tam3 copies on a single chromosome, in the three cases in which these rearrangements have been examined in detail in Antirrhinum, no evidence for copies of Tam3 at the reciprocal loci prior to rearrangement has been found; these rearrangements strongly support the arguments for a mechanism based on aberrant transposition (Lister and Martin, 1989; Robbins et al., 1989; this study).

This mechanism emphasizes two features of the transposition process: transposition must occur very shortly after replication to account for the close juxtapositioning of the replicated Tam3 copies, allowing their combined participation in the aberrant transposition; two opposite ends of the element must be closely associated throughout transposition whether they are from the same or from independent Tam3 copies. For the ends of two separate Tam3 copies to be integrated into the same recipient site, the transposition intermediate must involve a tight association of the two ends during excision and subsequent integration, implying their coordinated cutting and reintegration. A mechanism involving sequential transfer of the transposon ends does not imply such an association.

The close association of the two ends of a transposon during excision has also been proposed following the mapping of the binding sites of the *tnp*A gene product of the maize transposon *Supressor-mutator* (Gierl et al., 1988; Frey et al., 1990)

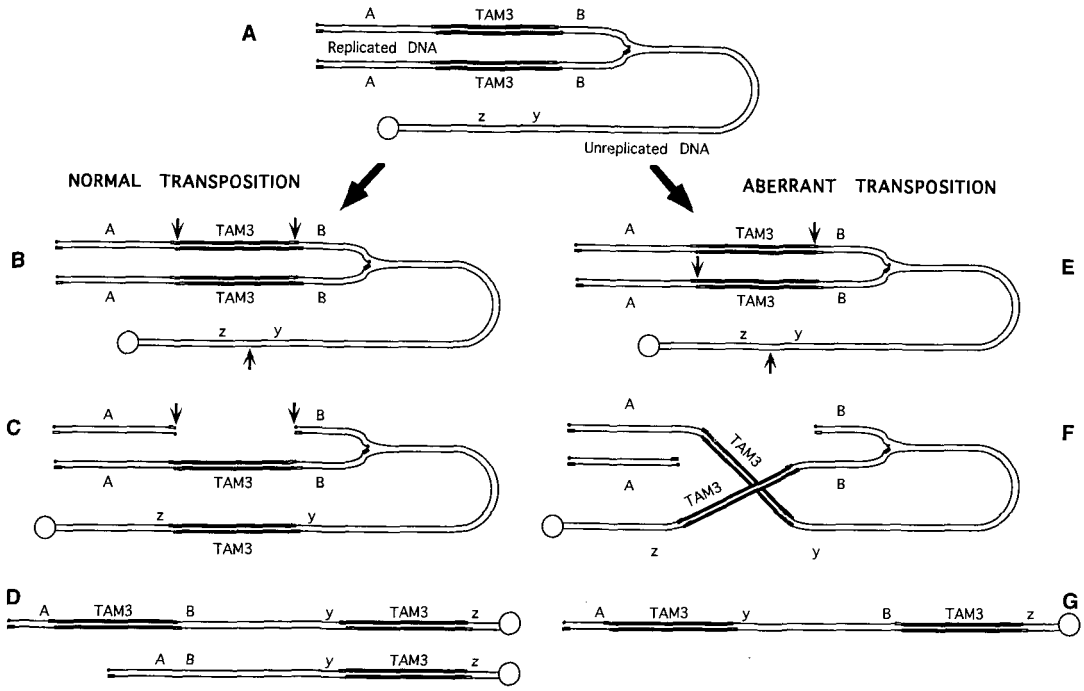

Figure 9. Models Describing a "Normal" and an "Aberrant" Transposition from which the Inversion at *niv*^{rec}:531 Might Have Arisen.

(A) Transposition occurs shortly after replication of the element.

(B) to **(D)** Normal transposition. In **(B)**, breakage occurs at each end of the of the same copy of Tam3 (at *niv*) and at a recipient site (*yz*). In **(C)**, the element is transferred to the recipient site; this is followed by ligation of the free ends at the donor site. In **(D)**, replication continues to produce two chromatids, one bearing a single copy of Tam3 and the other having two copies.

(E) to **(G)** Aberrant transposition. In **(E)**, breakage occurs at opposite ends of the replicated copies of Tam3 (at *niv*) and at the recipient site (*yz*); the element ends must be held together to allow the free ends of the elements to integrate at *yz*, as shown in **(F)**. In **(G)**, replication continues to produce one chromatid with a chromosomal inversion between the two copies of Tam3; the other chromosomal segments are lost through lack of a centromere.

and the *Activator* transposase (Feldmar and Kunze, 1991). The protein products bind to specific repeats in the subterminal repeated regions of both elements. In *Supressor-mutator*, if these repeat motifs in the two ends are aligned, the protein binding sites appear to interlock like the teeth of a "zipper," presumably stabilizing the alignment of the inverted repeats. The details of the aberrant transposition event that gave rise to *niv*^{rec}:531 support the view that the ends of the element remain tightly associated in vivo through both excision and integration.

Role of Tam3 in Modifying *nivea* Gene Expression

The inversion generated in *niv*^{rec}:531 displaces the *niv* promoter sequences upstream of −63 bp to a distance of more than 1 cM away from the −63 bp promoter and *niv* coding sequences. Deletion of these upstream sequences causes the loss of motifs required for *niv* expression in the upper part of the tube and reduces maximum steady state *niv* transcript levels by ~89%, as observed in JI:593. In situ hybridizations show that it does not cause a change in the specificity of expression in the epidermis. The motifs in *z* contribute to *niv* gene expression in JI:531R2, promoting it in the epidermis of the lobes by ~70% over that observed in JI:593 and directing expression to the adaxial part of the tube, but not the abaxial part.

The difference in the degree of pigmentation between the excision alleles *niv*:531R3 and *niv*:531R2 appears to be due to the sequences remaining from the original *niv* promoter. Partial loss of one of the TACCAT motifs in *niv*:531R3 reduces pigmentation relative to *niv*:531R2, confirming the results of Sommer et al. (1988a) that these motifs determine the strength of the *niv* promoter. Therefore, the remnant of the original *niv* promoter still plays a role in determining the level of gene expression driven by the chimeric promoter in these flowers.

Genetic analysis of the interaction of *niv*:531R2 with the *cyc* mutation suggests that region *z* binds a DNA binding factor or factors with abaxial/adaxial polarity in its or in their distribution. Such factors, which were functionally lost when their binding sites were displaced in the inversion of the upstream region of the *niv* promoter away from the gene, in *niv*^{rec}:531, might then substitute for those involved in activation of tube expression. These results imply that transcriptional regulation is an important component in the establishment of adaxial/

abaxial polarity in the flower. It may be possible to use JI:531 to explore this further, for example, to find the time during floral development at which polar control of *niv* expression is operational, and to use sequences within *z* to isolate the transcription factors involved in controlling polar expression. We also have strong circumstantial evidence that the sequences in *z* may normally control expression of a gene expressed in leaves and young buds, although we do not yet know whether this gene is regulated by *cyc* to any extent. The identification of the function of this gene may permit further insight into the determination of floral polarity in Antirrhinum.

In summary, analysis of JI:531 and its derivatives not only emphasizes the power of transposons to cause genomic structural changes but also illustrates the subtle changes in gene expression that can result from such genomic rearrangements.

METHODS

Antirrhinum majus Stocks

The *nivea* alleles, designated *niv*^{rec}:531 and *niv*:593, were derived from the *niv*^{rec}:98 allele of JI:98 (Harrison and Carpenter, 1979; Sommer et al., 1985; Carpenter et al., 1987; Martin et al., 1988) and have been maintained as homozygous lines JI:531 and JII:593. Wild-type line JI:7 (used for transcript analysis) and line JI:5A (used for restriction fragment length polymorphism [RFLP] analysis) were described by Harrison and Fincham (1964). JI:25 (*cycloidia*^{radialis} [*cyc*^{rad}]) was obtained from L. K. Crowe (Oxford) before 1963 and has been maintained as an inbred line since then.

Isolation of Antirrhinum Genomic DNA and Cloning of Plant Genomic DNA in λ EMBL4

Genomic DNA was prepared from frozen leaves as described by Martin et al. (1985). Genomic DNA (150 μg) was partially digested with EcoRI and size fractionated on a 0.6% agarose gel. Fragments between ~15 and 20 kb were isolated by electroelution (Maniatis et al., 1983). The λ EMBL4 EcoRI arms were prepared by digestion with EcoRI and BamHI, followed by isopropanol precipitation. Ligations between 500-ng vector arms and genomic fragments were optimized. The ligations were packaged in vitro and plated on *Escherichia coli* LE 392. Libraries were blotted onto nitrocellulose filters and screened with the appropriate fragments. For more detailed analysis, fragments were subcloned into pUC18 and M13 vectors for DNA sequence determination.

Phage DNA Preparation

Phage DNA was prepared from liquid lysates by PEG 6000 precipitation and purification on CsCl gradients and was followed by phenol/chloroform (1:1) extraction and ethanol precipitation, modified from the method of Will et al. (1981).

Plasmid DNA Preparation

Plasmid was prepared as described by Maniatis et al. (1983).

DNA Sequence Determination

Fragments to be sequenced were subcloned into the appropriate M13 (Yanisch-Perron et al., 1985) or pBluescript SK+ (Stratagene) vector. Template preparation, sequencing reactions (using ^{35}S-dATP), and buffer gradient electrophoresis were modified from the methods of Sanger et al. (1977) and Biggin et al. (1983).

Polymerase Chain Reactions

An oligonucleotide (B82) was prepared from the published *niv* sequence (Sommer and Saedler, 1986) from the region between the start of transcription and the start of translation downstream from a KpnI site. A second oligonucleotide (B80) was prepared from sequence ~1.6 kb away from *Tam3* in BT3z. Polymerase chain reaction (PCR) amplifications, using these oligonucleotides, were performed on genomic DNA from JI:531R1, JI:531R2, and JI:531R3 plus JI:98 as a control. PCR reactions were conducted using 0.5 μg of Antirrhinum genomic DNA in a 100-μL reaction volume containing 10 μL of 10 × reaction buffer (100 mM Tris-HCl, pH 8.3, 500 mM KCl, 15 mM $MgCl_2$; 0.1% [w/v] gelatine), 5 μL of each primer (20 mM stocks), 16 μL of nucleotide mix (1.2 5 mM for dATP, dCTP, dGTP, and dTTP), 0.1% Tween 20, and 2 units Amplitaq (Cetus Corp., Emeryville, CA) TaqI polymerase.

A program cycle consisting of 30 cycles of 94°C (15 sec) and followed by 46°C (15 sec), then 72°C (2 min) was used to amplify fragments of ~1.6 kb. At least three clones from each allele were sequenced to ensure that sequence alterations induced during PCR did not influence the sequences derived for the excision alleles.

RNA Preparation and Gel Blot Analysis

Total RNA and poly(A) RNA were isolated from dissected parts of flower petals, from buds, and from leaves by the methods described by Martin et al. (1985). Gel blot analysis of RNA separated on formaldehyde gels was performed as described by Martin et al. (1985), and the loading of gels was standardized using a cDNA probe encoding ubiquitin from Antirrhinum (K. Davies and C. Martin, unpublished results). Filters were washed twice with 0.1 × SSC (1 × SSC is 0.15 M NaCl, 0.015 M sodium citrate), 0.5% SDS at 65°C before exposure to Fuji R-X 100 film. Hybridization was quantified using a Joyce Loebl scanning densitometer. Primer extension was performed according to the methods of Sommer and Saedler (1986) and Maniatis et al. (1983).

In Situ Hybridization

In situ hybridization was performed on flower buds of 15 to 25 mm in length as described in Jackson et al. (1991). Riboprobes were labeled by incorporation of ^{3}H-UTP, and exposures were for between 2 and 4 weeks. As a control, a riboprobe of the *niv* sense strand was hybridized to sections of JI:531R2 flowers.

ACKNOWLEDGMENTS

We thank David Hopwood and George Coupland for critical appraisal of the manuscript and Enrico Coen and Eric Schoonejans for helpful discussions. We also thank Peter Scott, Andrew Davies, Nigel Hannant,

and Jim English for photography and figure preparation. C.L. and D.J. were supported by studentships from the John Innes Foundation.

Received June 7, 1993; accepted August 26, 1993.

REFERENCES

Biggin, M.D., Gibson, T.J., and Hong, G.F. (1983). Buffer gradient gels and ^{35}S label as an aid to rapid sequence determination. Proc. Natl. Acad. Sci. USA **80,** 3963–3965.

Boeke, J.D. (1989). Transposable elements in *Saccharomyces cerevisiae.* In Mobile DNA, D.E. Berg, and M.H. Howe, eds (Washington, DC: American Society for Microbiology), pp. 335–374.

Busseau, I., Pelisson, A., and Bucheton, A. (1989). I elements of *Drosophila melanogaster* generate specific chromosomal rearrangements during transposition. Mol. Gen. Genet. **218,** 222–228.

Carpenter, R., and Coen, E. (1990). Floral homeotic mutations produced by transposon-mutagenesis in *Antirrhinum majus.* Genes Dev. **4,** 1483–1493.

Carpenter, R., Martin, C., and Coen, E.S. (1987). Comparison of genetic behaviour of the transposable element Tam*3* at two unlinked loci in *Antirrhinum majus.* Mol. Gen. Genet. **207,** 82–89.

Chen, J., Greenblatt, I.M., and Dellaporta, S. (1987). Transposition of *Ac* from the *P* locus of maize into unreplicated chromosomal sites. Genetics **117,** 109–116.

Coen, E.S., and Carpenter, R. (1988). A semi-dominant allele, *niv*:525, acts in *trans* to inhibit expression of its wild-type homologue in *Antirrhinum majus.* EMBO. J. **7,** 877–883.

Coen, E.S., Carpenter, R., and Martin, C. (1986). Transposable elements generate novel spatial patterns of gene expression in *Antirrhinum majus.* Cell **47,** 285–296.

Dooner, H., English, J., and Ralston, E. (1988). The frequency of transposition of the maize element *Activator* is not affected by an adjacent deletion. Mol. Gen. Genet. **211,** 485–491.

Engels, W.R., and Preston, C.R. (1984). Formation of chromosome rearrangements by P factors in *Drosophila.* Genetics **107,** 657–678.

Feldmar, S., and Kunze, R. (1991). The ORFa protein, the putative transposase of maize transposable element *Ac,* has a basic DNA binding domain. EMBO J. **10,** 4003–4010.

Frey, M., Reinecke, J., Grant, S., Saedler, H., and Gierl, A. (1990). Excision of the *En/Spm* transposable element of *Zea mays* requires two element-encoded proteins. EMBO J. **9,** 4037–4044.

Gierl, A., Lütticke, S., and Saedler, H. (1988). *TnpA* product encoded by the transposable element *En-1* of *Zea mays* is a DNA binding protein. EMBO J. **7,** 4045–4053.

Greenblatt, I.M. (1984). A chromosome replication pattern deduced from pericarp phenotypes resulting from movements of the transposable element *Modulator* in maize. Genetics **108,** 471–485.

Greenblatt, I.M., and Brink, R.A. (1962). Twin mutations in medium variagated pericarp maize. Genetics **47,** 489–501.

Harrison, B.J., and Carpenter, R. (1968). John Innes Annual Report (Norwich, UK: John Innes Institute), pp. 40–45.

Harrison, B., and Carpenter, R. (1979). Resurgence of genetic instability in *Antirrhinum majus.* Mutat. Res. **63,** 47–66.

Harrison, B., and Fincham, J.R.S. (1964). Instability at the *pal* locus in *Antirrhinum majus.* I. Effects of environment on frequencies of somatic and germinal mutation. Heredity **19,** 237–258.

Harrison, B., and Fincham, J.R.S. (1968). Instability at the *pal* locus in *Antirrhinum majus.* III. A gene controlling mutation frequency. Heredity **23,** 67–72.

Hehl, R., Nacken, W.F.G., Krause, A., Saedler, H., and Sommer, H. (1991). Structural analysis of Tam*3*, a transposable element of *Antirrhinum majus,* reveals homologies to the *Ac* element from maize. Plant Mol. Biol. **16,** 369–371.

Hudson, A.D., Carpenter, R., and Coen, E.S. (1990). Phenotypic effects of short-range and aberrant transposition in *Antirrhinum majus.* Plant Mol. Biol. **14,** 835–844.

Jackson, D. (1992). *In situ* hybridisation in plants. In Molecular Plant Pathology: A Practical Approach, D.J. Bowles, S.J. Gurr, and M. McPherson, eds (Oxford: Oxford University Press), pp. 163–174.

Jones, J.D.G., Carland, F., Lim, E., Ralston, E., and Dooner, H.K. (1990). Preferential transposition of the maize element *Activator* to linked chromosomal locations in tobacco. Plant Cell, **2,** 701–707.

Kaulen, H., Schell, J., and Kreuzaler, F. (1986). Light-induced expression of the chimeric chalcone synthase-NPTII gene in tobacco cells. EMBO J. **5,** 1–8.

Kleckner, N., and Ross, D.G. (1980). *Rec*A-dependent switch generated by transposon Tn*10.* J. Mol. Biol. **144,** 215–221.

Kunze, R., and Starlinger, P. (1989). The putative transposase of transposable element *Ac* from *Zea mays* L. interacts with subterminal sequences of *Ac.* EMBO J. **8,** 3177–3185.

Lipphardt, S., Brettschneider, R., Kreuzaler, F., Schell, J., and Dangl, J. (1988). UV-inducible transient expression in parsley protoplasts identifies regulatory *cis*-elements of a chimeric *Antirrhinum majus* chalcone synthase gene. EMBO J. **7,** 4027–4033.

Lister, C., and Martin, C. (1989). Molecular analysis of a transposon-induced deletion of the *nivea* locus in *Antirrhinum majus.* Genetics **123,** 417–425.

Maniatis, T., Fritsch, E.F., and Sambrook, J. (1983). Molecular Cloning: A Laboratory Manual. (Cold Spring Harbor, NY: Cold Spring Harbor Laboratory Press).

Martin, C., and Lister, C. (1989). Genome juggling by transposons: Tam*3*-induced rearrangements in *Antirrhinum majus.* Dev. Genetics **10,** 438–451.

Martin, C., Carpenter, R., Sommer, H., Saedler, H., and Coen, E.S. (1985). Molecular analysis of instability in flower pigmentation of *Antirrhinum majus,* following isolation of the *pallida* locus by transposon tagging. EMBO J. **4,** 1625–1630.

Martin, C., MacKay, S., and Carpenter, R. (1988). Large-scale chromosomal restructuring is induced by the transposable element Tam*3* at the *nivea* locus of *Antirrhinum majus.* Genetics **119,** 171–184.

Martin, C., Prescott, A., Lister, C., and MacKay, S. (1989). Activity of the transposon Tam*3* in *Antirrhinum* and tobacco: Possible role of DNA methylation. EMBO J. **8,** 997–1004.

Robbins, T., Carpenter, R., and Coen, E.S. (1989). A chromosome rearrangement suggests that donor and recipient sites are associated during Tam*3* transposition in *Antirrhinum majus.* EMBO J. **8,** 5–13.

Roeder, G.S., and Fink, G.R. (1983). Transposable elements in yeast. In Mobile Genetic Elements, J. Shapiro, ed (New York: Academic Press), pp. 299–328.

Sanger, F., Nicklen, S., and Coulsen, A.R. (1977). DNA sequencing with chain-terminating inhibitors. Proc. Natl. Acad. Sci. USA **74,** 5463–5467.

Schulze-Lefert, P., Dangl, J., Becker-André, M., Hahlbrock, K., and Schulz, W. (1989a). Inducible *in vivo* DNA footprints define sequences necessary for UV light activation of the parsley chalcone synthase gene. EMBO J. **8,** 651–656.

Schulze-Lefert, P., Becker-André, M., Schulz, W., Hahlbrock, K. and Dangl, J.L. (1989b). Functional architecture of the light-responsive chalcone synthase promoter from parsley. Plant Cell **1,** 707–714.

Sommer, H., and Saedler, H. (1986). Structure of the chalcone synthase gene of *Antirrhinum majus.* Mol. Gen. Genet. **202,** 429–434.

Sommer, H., Carpenter, R., Harrison, B.J., and Saedler, H. (1985). The transposable element Tam3 of *Antirrhinum majus* generates a novel type of sequence alterations upon excision. Mol. Gen. Genet. **199,** 225–231.

Sommer, H., Bonas, U., and Saedler, H. (1988a). Transposon-induced alterations in the promoter region affect transcription of the chalcone synthase gene of *Antirrhinum majus.* Mol. Gen. Genet. **211,** 49–55.

Sommer, H., Hehl, R., Krebbers, E., Piotrowiak, R., Lonning, W.-E., and Saedler, H. (1988b). Transposable elements of *Antirrhinum majus.* In Plant Transposable Elements, O. Nelson, ed (New York: Plenum Press), pp. 227–235.

Stubbe, H. (1966). Genetik und Zytologie von *Antirrhinum* L. sect. *Antirrhinum* (Jena, Germany: Veb. Gustav Fischer Verlag).

Taylor, L.P., and Walbot, V. (1985). A deletion adjacent to the maize transposable element *Mu-1* accompanies loss of *Adh* expression. EMBO J. **4,** 869–876.

Van Schaik, N.W., and Brink, R.A. (1959). Transpositions of *Modulator,* a component of the *variegated pericarp* allele in maize. Genetics **44,** 725–738.

Will, B.M., Bayev, A.A., and Finnegan, D.J. (1981). Nucleotide sequence of terminal repeats of 412 transposable elements of *Drosophila melanogaster.* J. Mol. Biol. **153,** 897–915.

Yanisch-Perron, C., Vieira, J., and Messing, J. (1985). Improved M13 phage cloning vectors and host strains: Nucleotide sequences of the M13mp18 and pUC19 vectors. Gene **33,** 103–119.